

Intercombination transition rates in N^+

Xiaozhi Shen*

*School of Mechanical and Electrical Engineering, Handan University, Handan 056005, China
and School of Physics and Nuclear Energy Engineering, Beihang University, Beijing 100191, China*

Juan Liu†

*School of Mathematics and Physics, Handan University, Handan 056005, China
and School of Information, Renmin University of China, Beijing 100872, China*

Cuicui Sang

*College of Science, Lanzhou University of Technology, Lanzhou 730050, China
and Department of Physics, Qinghai Normal University, Xining 81001, China*

Per Jönsson‡

Materials Science and Applied Mathematics, Malmö University, 205 06 Malmö, Sweden

(Received 20 November 2017; published 22 January 2018)

Accurate intercombination transition rates (A), arising from the $2s^2 2pnl$ ($n = 3, 4, 5$; $l = s, p, d$) and $2s2p^3$ configurations of N^+ , are reported. Wavefunctions for the studied states in N^+ are determined using the multiconfiguration Dirac-Hartree-Fock (MCDHF) method and account for the effects of valence, core-valence (CV), and core-core (CC) correlations. It is found that the combined CV and CC correlation effects are important for accurate predictions of intercombination rates of N^+ . A strong spin-orbit mixing between the states $^3P_1^o$ and $^1P_1^o$ of $2s^2 2p3s$ causes that the intercombination rates on its states $^{1,3}P_1^o$ are exceedingly sensitive to electron correlations and other corrections. The strong visible intercombination lines of N^+ arise from the $2s^2 2p3s-2s^2 2p3p$ and $2s^2 2p3p-2s^2 2p3d$ transitions. There are also strong infrared and ultraviolet intercombination lines that have important applications in plasma diagnosis of radiative cooling coefficient and abundance. Different systematic methods are used to evaluate the intercombination rates and their uncertainties. For relatively strong lines ($gf > 0.01$) of $2s^2 2p3l$ ($l = s, p, d$), $2s^2 2p4l$ ($l = s, p, d$) and $2s^2 2p5s$ the uncertainties are separately estimated to be within 7%, 12%, and 20%. The rates of extremely weak lines, $gf < 10^{-6}$, are of interests in the temperature and density diagnostic in nebulae, but are remarkably difficult to accurately calculate. The present calculations have included appropriate electron correlations to deal with them and provide guidance for further studies.

DOI: [10.1103/PhysRevA.97.012510](https://doi.org/10.1103/PhysRevA.97.012510)

I. INTRODUCTIONS

Nitrogen is one of the most abundant elements in the universe. The rates (A) of the intercombination transitions in singly ionized nitrogen (N^+) are of interests in plasma diagnostics of electron temperature (Te), electron density (Ne), radiative cooling coefficient, etc. [1–8]. For example, Tripp *et al.* reported that the intercombination line $\lambda 74.84$ nm is anomalously strong [1], and that the rate is important for the diagnostics of radiative cooling coefficient and Te in the upper atmospheres of Earth and Titan [1,9]. The determination of Te and Ne in the Orion Nebula was independently done by Rubin *et al.* [2] and Keenan *et al.* [3] using the $2s^2 2p^2 \ ^3P_{1,2}-2s2p^3 \ ^5S_2^o$ intercombination lines. Ahmed and Sigut pointed out that intercombination rates of N^+ can be used for abundance

calculation and analysis [8]. Many intercombination lines of $2s^2 2p3s-2s^2 2p3p$ and $2s^2 2p3p-2s^2 2p3d$, excited by fluorescence light in the Orion Nebula, were observed by Escalante and Morisset [4]. In all, accurate intercombination data are desired for reliable plasma diagnostics.

The experimental methods for determining intercombination rates of N^+ depend on the type of transition. The $2s^2 2p3s-2s^2 2p3p$ and $2s^2 2p3p-2s^2 2p3d$ transitions fall in the visible region with relatively strong intensities [10,11], and their rates have been determined by Musielok [10] and Mar [11] based on measurements in discharge plasmas. Many strong intercombination lines fall in the infrared and ultraviolet regions. They have valuable applications in plasma diagnosis [1,12], but the experimental rates were seldom reported, e.g., that of $\lambda 51.452$ nm, $\lambda 63.065$ nm, $\lambda 1332.797$ nm, $\lambda 1386.647$ nm, etc. Measurements of transition rates from the metastable state $2s2p^3 \ ^5S_2^o$ require other methods, as its rates are tiny and the corresponding lifetime in this case is of the order of milliseconds [13–17]. Under these cases theoretical calculations can be given more attention.

*shenzx@buaa.edu.cn

†juanliu@ruc.edu.cn

‡per.jonsson@mah.se

TABLE I. The number of CSFs (N_{CSFs}) for different angular momenta (J) and parities in different computational models. AS denotes the highest principal quantum number n in the active set of orbitals. DHF stands for the calculations based on the CSFs of the reference configurations. nSDV, nSDVC, nSDVCB, and nSDVCBQ denote the computational models as described in the text.

Reference configurations	AS	Models	N_{CSFs}					
			$J = 0$	$J = 1$	$J = 2$	$J = 3$	$J = 4$	$J = 5$
		Even						
$\{2s^2 2p^2; 2s^2 2p^3 p; 2s^2 2p^4 p; 2s^2 2p^2 3s; 2s^2 2p^4 f;$ $2s^2 3d^2; 2s^2 2p^2 3d; 2s^2 2p^3 p 3d; 2s^2 3s 3d^2; 2p^4; 2p^3 3p; 2p^2 3s 3d\}$		DHF	41	89	106	77	42	13
	4	4SDV	906	2297	3020	2841	2193	1371
	5	5SDV	3064	8167	11 296	11 736	10 251	7625
	6	6SDV	7172	19 603	28 028	30 878	29 098	23 950
	7	7SDV	13 808	38 369	56 239	64 626	64 425	57 154
$\{1s^2 2s^2 2p^2; 1s^2 2s^2 2p^3 p; 1s^2 2s^2 2p^4 p;$ $1s^2 2s^2 2p^2 3s; 1s^2 2s^2 2p^4 f\}$	7	7SDVC	71 635	200 660	294 281	339 943	339 811	303 282
	7	7SDVCB	71 635	200 660	294 281	339 943	339 811	303 282
$\{1s^2 2s^2 2p^2; 1s^2 2s^2 2p^3 p; 1s^2 2s^2 2p^4 p;$ $1s^2 2s^2 2p^2 3s; 1s^2 2s^2 2p^4 f; 1s^2 2p^4\}$	7	7SDVCBQ	75 556	211 321	309 751	357 244	356 620	317 640
		Odd						
$\{2s^2 p^3; 2s^2 2p^3 s; 2s^2 2p^3 d; 2s^2 2p^4 s; 2s^2 2p^4 d; 2s^2 2p^5 s\}$		DHF	6	16	15	7	2	
	4	4SDV	1033	2727	3463	3230	2406	
	5	5SDV	3035	8255	11 231	11 606	9917	
	6	6SDV	7109	19 682	27 856	30 598	28 473	
	7	7SDV	13 609	38 147	55 462	63 516	62 654	
$\{1s^2 2s^2 2p^3; 1s^2 2s^2 2p^3 s; 1s^2 2s^2 2p^3 d;$ $1s^2 2s^2 2p^4 s; 1s^2 2s^2 2p^4 d; 1s^2 2s^2 2p^5 s\}$	7	7SDVC	68 459	192 172	280 405	322 427	319 636	
	7	7SDVCB	68 459	192 172	280 405	322 427	319 636	
	7	7SDVCBQ	68 459	192 172	280 405	322 427	319 636	

Accurate calculations of intercombination transitions of N^+ remain a challenge due to the strong influence of electron correlation effects on the transition matrix elements. Two CIV3 calculations of $2s^2 2p^3 s - 2s^2 2p n p$ ($n = 3, 4$) by Bell *et al.* [18] and Vaecck *et al.* [19] show that the correlation of $\{6s, 6p\}$ orbitals can affect the intercombination rates roughly by a factor of two. Importance of correlation of $\{7s, 7p, 6d-7d, 6f-7f, 6h-7h, 7i\}$ orbitals for intercombination rates has been also confirmed [13,20]. In addition, the effects of core-valence (CV) and core-core (CC) correlations were seldom included in the past, especially not for calculations of the intercombination rates from $2s^2 2p n l$ ($n \geq 3$) [18,21–28]. Tayal found the influence of CV correlation effects for the intercombination rates of N^+ is insignificant [28]. But the studies on the influences of combined CV and CC correlations for these rates are considerable scarce. Tayal reported strong interactions between $2s^2 2p^3 \ ^1,^3P_1^o$ and $2s^2 2p^3 s \ ^1,^3P_1^o$ [28], just as Ellis did [12]. However, they restricted their reference configurations to $\{2s^2 p^3, 2s^2 2p^3 s, 2s^2 2p^3 d\}$ [12,26,28], which neglected some important correlation effects. Accurately calculating the intercombination rates involving two-electron-one-photon processes is not easy. For example, those of $2s^2 p^3 \ ^3P^o - 2s^2 2p^4 p$ [13], higher-order correlation effects [29] are enhanced as the rates are identically zero in the single configuration approximation. The effects of the Breit interaction are also very important for calculations of intercombination rates [30]. Illustrative examples are given by the calculations of the small rates arising from $2s^2 p^3 \ ^5S_2^o$ [13]. In all, solving these issues is valuable, even urgent, considering the fact that accurate experimental intercombination rates are scarce [10,11,14–17].

II. THEORETICAL METHOD AND COMPUTATIONAL MODELS

A. Theoretical method

The atomic state wavefunctions (ASFs) can be generated by using the MCDHF method [31,32]. The ASFs are linear combinations of configuration state functions (CSFs) with same parity P , angular momentum J , and its z component M_J :

$$\Psi(PJM_J) = \sum_{j=1}^N c_j \Phi(\gamma_j P J M_J). \quad (1)$$

Here, c_j and γ_j are, respectively, the mixing coefficient and other appropriate labeling of the CSFs built from products of one-electron Dirac orbitals. The self-consistent field (SCF) method was employed to optimize the radial parts of the Dirac orbitals and the expansion coefficients, and an extended optimal level (EOL) scheme was further applied to obtain balanced energies for the studied states. The Breit interaction,

$$B_{ij} = -\frac{1}{2r_{ij}} \left[\vec{\alpha}_i \cdot \vec{\alpha}_j + \frac{(\vec{\alpha}_i \cdot \vec{r}_{ij})(\vec{\alpha}_j \cdot \vec{r}_{ij})}{r_{ij}^2} \right], \quad (2)$$

as well as the quantum electrodynamics (QED) effects, including self-energy and vacuum polarization, were included in subsequent relativistic configuration interaction (RCI) calculations [31].

The electric dipole transition rate from an upper state u to a lower one l can be written [33]

$$A = \frac{4}{3} \alpha \frac{(E_u - E_l)^3}{\hbar^3 c^2} \frac{S}{2J_u + 1}, \quad (3)$$

TABLE II. The excitation energies (E) with $J = 1$ in N⁺, δ_E , and the energy difference in different correlation models (ΔE). $\Delta E_{CV\&CC}$ and ΔE_{Breit} are corresponding to the energy difference of ($E_{7SDVC} - E_{7SDV}$) and ($E_{7SDVCB} - E_{7SDVC}$), respectively.

Levels	$E(\text{cm}^{-1})$			$100\delta_E$		$\Delta E(\text{cm}^{-1})$	
	Present	MCHF ^a	NIST ^b	Present	MCHF ^a	$\Delta E_{CV\&CC}$	ΔE_{Breit}
$2s^2 2p^2 \ ^3P_1$	49	41	49	0.06	16.63	0	-7
$2s 2p^3 \ ^3D_1^o$	92 335	92 655	92 252	0.09	0.44	-544	-25
$2s 2p^3 \ ^3P_1^o$	109 425	109 982	109 217	0.19	0.70	-454	-30
$2s^2 2p 3s \ ^3P_1^o$	148 804	149 081	148 940	0.09	0.09	212	-21
$2s^2 2p 3s \ ^1P_1^o$	149 101	149 254	149 188	0.06	0.04	152	-43
$2s 2p^3 \ ^3S_1^o$	155 685	156 112	155 127	0.36	0.64	-1187	-35
$2s^2 2p 3p \ ^1P_1$	164 532	164 649	164 611	0.05	0.02	399	-34
$2s^2 2p 3p \ ^3D_1$	166 438	166 586	166 522	0.05	0.04	399	-19
$2s 2p^3 \ ^1P_1^o$	167 621	168 686	166 766	0.51	1.15	-720	-34
$2s^2 2p 3p \ ^3S_1$	168 771	169 024	168 892	0.07	0.08	404	-34
$2s^2 2p 3p \ ^3P_1$	170 458	170 701	170 608	0.09	0.05	378	-30
$2s^2 2p 3d \ ^3D_1^o$	187 197	187 499	187 438	0.13	0.03	209	-34
$2s^2 2p 3d \ ^3P_1^o$	188 683	188 977	188 909	0.12	0.04	213	-45
$2s^2 2p 3d \ ^1P_1^o$	189 982	190 259	190 120	0.07	0.07	209	-41
$2s^2 2p 4s \ ^3P_1^o$	196 364		196 592	0.12		214	-27
$2s^2 2p 4s \ ^1P_1^o$	197 651		197 859	0.10		178	-41
$2s^2 2p 4p \ ^1P_1$	202 050		202 171	0.06		423	-34
$2s^2 2p 4p \ ^3D_1$	202 561		202 714	0.08		420	-22
$2s^2 2p 4p \ ^3P_1$	202 969		203 189	0.11		360	-29
$2s^2 2p 4p \ ^3S_1$	203 356		203 538	0.09		418	-41
$2s 2p^2 3s \ ^5P_1$	205 069		205 598	0.26		-227	-19
$2s^2 2p 4d \ ^3D_1^o$	209 969		210 240	0.13		207	-32
$2s^2 2p 4d \ ^3P_1^o$	210 479		210 751	0.13		210	-47
$2s^2 2p 4d \ ^1P_1^o$	211 129		211 336	0.10		283	-43
$2s^2 2p 4f \ D(3/2)_1$	211 267		211 487	0.10		360	-48
$2s^2 2p 5s \ ^3P_1^o$	213 990		214 258	0.13		209	-26
$2s^2 2p 5s \ ^1P_1^o$	214 566		214 829	0.12		198	-44

^aTayal [28].

^bCiting from Ref. [38].

where α , $E_u - E_l$ (or ΔE), and S are, respectively, the fine structure constant, the transition energy, and the line strength. The line strength can be given in the Babushkin and Coulomb gauges [34], which in the nonrelativistic limit correspond to the length and velocity gauges [33,35]. The line strengths in the Babushkin gauge are to first order independent of the transition energies ΔE . More accurate transition rates, which we refer to as adjusted transition rates A_{adj} , can be obtained by scaling the calculated transition rates A_{calc} with the ratio of the observed ΔE_{obs} and calculated ΔE_{calc} transition energies to compensate for some of the neglected correlation effects. A similar scaling can be also done for the weighted oscillator strengths gf . Denoting the energy ratio by $r = \Delta E_{\text{obs}}/\Delta E_{\text{calc}} = \lambda_{\text{calc}}/\lambda_{\text{obs}}$ we have $A_{(\text{adj})} = r^3 A_{(\text{calc})}$ and $gf_{(\text{adj})} = r gf_{(\text{calc})}$ [26]. The above scaling is only valid in the Babushkin gauge. The impact for A affected by this scaling correction obviously appear in the case of extremely small ΔE (or very large λ) [20]. A biorthogonal transformation technique is needed so that standard Racah algebra can be used for evaluating transition matrix elements between states with different orthonormal orbital sets [36]. The

latest version of the GRASP2K package was used for all the calculations [37].

B. Computational models

The computational procedures are summarized in Table I. The multireference configurations (MR) for the odd and even parity states were taken as $\{2s 2p^3, 2s^2 2p 3s, 2s^2 2p 3d, 2s^2 2p 4s, 2s^2 2p 4d, 2s^2 2p 5s\}$ and $\{2s^2 2p^2, 2s^2 2p 3p, 2s^2 2p 4p, 2s 2p^2 3s, 2s^2 2p 4f\}$, respectively. The orbitals of these 11 configurations were treated as occupied orbitals. The CSFs were formed from all configurations that could be obtained by single (S) and double (D) substitutions of the occupied orbitals in the MR with orbitals in an active set. The active sets for the odd and even parity states were extended layer by layer so as to be able to monitor the convergence, and systematically enlarged to include orbitals with principal quantum numbers $n = 2 \sim 7$, and orbital quantum numbers $l = 0 \sim 6$ (i.e., angular symmetries s, p, d, f, g, h, i). Here, except for occupied orbitals others are treated as correlation

TABLE III. Wavelengths (λ), line strengths (S), weighted oscillator strengths (gf), and transition rates (A) of some $2s^2 2pnl(n \geq 3)$ intercombination lines of N^+ . Calc. and Obs. represent the calculated and observed results, respectively. Exp. is experiment. The number in square bracket represents the power of 10.

Lower	Upper	$\lambda(\text{nm})$		S	gf	$A(s^{-1})$								
		Calc.	Obs. ^a			Present	CIV3		MCHF		Exp.			
							Bell ^b	Vaeck ^c	Fischer ^d	Ellis ^e	Tayal ^f	Musielok ^g	Mar ^h	
$2s^2 2p^2 \ ^3P_0$	$2s^2 2p3s \ ^1P_1^o$	67.069	67.030	1.20[-2]	5.45[-3]	2.69[7]	1.85[7]		3.80[7]	3.50[7]				
	$\ ^3P_1$	67.091	67.051	9.61[-3]	4.36[-3]	2.15[7]	1.51[7]		3.02[7]	2.50[7]				
	$\ ^3P_2$	67.127	67.088	1.13[-2]	5.10[-3]	2.52[7]	1.60[7]		3.68[7]	4.40[7]				
	$\ ^1D_2$	74.997	74.837	1.68[-1]	6.83[-2]	2.71[8]	1.92[8]		3.81[8]	3.74[8]				
$2s^2 2p3s \ ^3P_1^o$	$2s^2 2p3p \ ^1S_0$	337.869	340.911	2.67[-1]	2.38[-2]	1.36[7]	9.38[6]	1.85[7]	1.91[7]		2.21[7]	2.36 ± 0.33[7]		
	$\ ^3P_1^o$	393.989	395.697	1.35[0]	1.04[-1]	8.86[6]	6.02[6]	1.19[7]	1.21[7]		1.50[7]	1.33 ± 0.11[7]	1.29[7]	
	$\ ^1P_1^o$	466.955	465.583	3.52[-1]	2.30[-2]	1.41[6]	9.58[5]	1.95[6]	1.92[6]		2.40[6]	2.72 ± 0.25[6]	2.2[6]	
	$\ ^1P_1^o$	468.224	466.851	2.64[-1]	1.72[-2]	1.75[6]	1.25[6]	2.33[6]	2.31[6]		2.84[6]	3.48 ± 0.32[6]		
	$\ ^1P_1^o$	468.991	467.622	3.21[-1]	2.09[-2]	6.36[6]	4.40[6]	8.64[6]	8.53[6]		1.06[7]	1.16 ± 0.10[7]		
	$\ ^1P_1^o$	508.394	507.501	3.43[-1]	2.05[-2]	1.77[6]	1.25[6]	2.29[6]	2.43[6]		2.76[6]	2.67 ± 0.21[6]	2.9[6]	
	$\ ^1P_1^o$	574.718	574.889	1.12[0]	5.90[-2]	2.38[6]	1.65[6]	3.47[6]	3.27[6]		3.59[6]	3.32 ± 0.32[6]		
	$\ ^1P_1^o$	576.816	576.905	5.29[-1]	2.78[-2]	1.86[6]	1.33[6]	2.53[6]	2.39[6]		2.62[6]	2.29 ± 0.21[6]		
	$\ ^3P_1^o$	635.801	638.138	1.06[0]	5.05[-2]	2.75[6]	1.95[6]	3.48[6]	3.52[6]		4.45[6]	6.11 ± 0.7[6]	4.9[6]	
$2s^2 2p^2 \ ^3P_1$	$2s^2 2p3d \ ^1D_2^o$	53.518	53.464	1.05[-2]	5.98[-3]	2.79[7]	2.18[7]		2.62[7]					
	$\ ^1D_2$	58.221	58.090	7.13[-3]	3.73[-3]	1.47[7]	1.24[7]		1.38[7]					
	$\ ^1D_2$	58.527	58.413	1.44[-2]	7.47[-3]	2.92[7]	2.06[7]		2.35[7]					
$2s^2 2p3p \ ^1P_1$	$\ ^3F_2^o$	458.821	456.604	4.57[-1]	3.04[-2]	1.94[6]	1.41[6]		1.65[6]				1.9[6]	
	$\ ^3D_1$	488.656	486.152	6.22[-1]	3.88[-2]	2.19[6]	1.61[6]		1.87[6]				1.7[6]	
$2s2p^3 \ ^3S_2^o$	$2s^2 2p4p \ ^1D_2$	62.968	63.065	6.38[-1]	3.07[-1]	1.03[9]								
$2s^2 2p3d \ ^3F_2^o$	$\ ^1P_1$	636.030	638.608	3.98[-1]	1.89[-2]	1.03[6]	7.86[5]							
	$\ ^1D_2^o$	638.595	640.092	4.88[-1]	2.31[-2]	1.26[6]	9.48[5]							
$2s^2 2p4s \ ^3P_1^o$	$\ ^1P_1$	1758.653	1792.577	1.85[0]	3.13[-2]	2.17[5]	1.79[5]							
	$\ ^3P_1$	1880.399	1876.053	6.48[-1]	1.05[-2]	6.62[4]	4.22[4]							
	$\ ^1P_1^o$	2036.627	2059.550	1.15[0]	1.70[-2]	8.93[4]	8.43[4]							
$2s^2 2p^2 \ ^3P_0$	$2s^2 2p4d \ ^1P_1^o$	47.364	47.318	1.76[-3]	1.13[-3]	1.12[7]								
	$\ ^3P_1$	47.699	47.647	1.17[-2]	7.46[-3]	4.38[7]								
	$\ ^1D_2$	51.405	51.295	4.77[-3]	2.83[-3]	1.43[7]								
	$\ ^1D_2$	51.548	51.452	2.26[-2]	1.33[-2]	6.73[7]								
$2s^2 2p4p \ ^3D_1$	$\ ^1P_1^o$	1167.104	1159.818	5.96[-1]	1.56[-2]	2.58[5]								
	$\ ^1P_1$	1258.039	1235.268	9.55[-1]	2.35[-2]	2.05[5]								
	$\ ^1P_1$	1262.703	1239.280	9.91[-1]	2.43[-2]	3.52[5]								
	$\ ^1P_1$	1349.713	1332.797	1.37[1]	3.12[-1]	2.34[6]								
	$\ ^3D_1$	1401.033	1386.647	1.67[1]	3.65[-1]	2.53[6]								
$2s^2 2p4p \ ^3D_1$	$2s^2 2p5s \ ^1P_1^o$	832.971	825.419	6.05[-1]	2.23[-2]	7.27[5]								
	$\ ^1P_1$	837.535	827.331	1.39[0]	5.10[-2]	1.66[6]								
	$\ ^3D_2$	836.337	828.918	4.82[-1]	1.77[-2]	5.71[5]								
	$\ ^3P_1$	862.271	859.095	4.98[-1]	1.76[-2]	5.30[5]								

^aReference [38].^bReference [18].^cReference [19].^dReference [26].^eReference [12].^fReference [28].^gReference [10].^hReference [11].

TABLE IV. (a) λ and A of some $2s^22p^2-2s2p^3$ intercombination lines. (b) The Branching Ratio (BR) of $2s2p^3\ ^5S_2^o$.

Tab	$2s^22p^2$	$2s2p^3$	$\lambda(\text{nm})$		A and BR				
			Calc.	Obs. ^a	Present	MCDHF ^b	MCHF		Exp.
							Fischer ^c	Tayal ^d	
(a) A (s^{-1})									
1	1D_2	$^5S_2^o$	324.181	317.779	9.83[−3]	1.40[−3]	8.95[−4]		
2	3P_1	$^5S_2^o$	216.153	213.968	4.02[1]	4.47[1]	5.16[1]	4.70[1]	
3	1D_2	$^3D_1^o$	130.090	129.979	3.21[2]	4.84[2]	5.93[2]		
4	3P_2	$^5S_2^o$	216.533	214.345	9.90[1]	1.10[2]	1.27[2]	1.16[2]	
5	1S_0	$^3D_1^o$	168.148	167.889	6.00[2]	3.78[2]	3.62[2]		
6	3P_2	$^1P_1^o$	59.705	60.011	5.34[3]		3.15[4]		
7	1D_2	$^3D_2^o$	130.090	129.981	8.77[2]	7.86[2]	7.33[2]		
8	1S_0	$^3P_1^o$	130.613	130.671	2.36[3]	2.01[3]	2.06[3]		
9	3P_0	$^1P_1^o$	59.658	59.964	1.71[4]		1.02[4]		
10	1D_2	$^3P_1^o$	106.428	106.496	5.68[3]	5.41[3]	5.16[3]		
11	1D_2	$^3P_2^o$	106.432	106.495	3.41[3]	1.93[3]	2.30[3]		
12	1S_0	$^3S_1^o$	81.419	81.674	1.23[4]		1.85[4]		
13	1D_2	$^3D_3^o$	130.108	130.004	4.42[3]	4.09[3]	4.14[3]		
14	3P_2	$^1D_2^o$	69.013	69.417	3.10[4]	1.18[5]	4.14[4]		
15	3P_1	$^1P_1^o$	59.676	59.982	1.33[5]		1.70[5]		
16	1D_2	$^3S_1^o$	71.317	71.525	1.16[5]		1.06[5]		
(b) The BR of $\frac{A_{\lambda 214,345}}{A_{\lambda 213,968}}$									
					2.462	2.461	2.456	2.462	2.45 ± 0.07^e
									2.24 ± 0.06^f

^aReference [38].^bJönsson and Bieroń [39].^cReference [26].^dReference [28].^eBridges *et al.* [40].^fMusielok *et al.* [10].

orbitals. For the SCF calculations the $1s^2$ core is kept closed and the generated CSF expansions account for valence (V) correlation. We denoted the computational model above by nSDV.

The CV and CC correlation effects were accounted for in RCI calculations [37] by allowing, respectively, S and D substitutions also from the $1s^2$ core. The corresponding computational model applied to the largest orbital set is denoted 7SDVC. It is known that the Breit interaction is important for intercombination transitions and this interaction along with QED effects were also included in RCI for the largest orbital sets. When including Breit and QED we refer to the models as 7SDVCB and 7SDVCBQ, respectively. Note that for the even states in Table I, adding $\{2p^4\}$ into the MR in the nSDV($n = 4 \sim 7$) models does not increase the number of CSFs; all CSFs obtained by SD substitutions from $\{2p^4\}$ are also obtained by SD substitutions from $\{2s^22p^2\}$. Things differ when opening $1s^2$. Adding $\{1s^22p^4\}$ to the MR for the 7SDVCBQ model increases the number of CSFs compared to the 7SDVCB model. Thus, the 7SDVCB and 7SDVCBQ models differ in both the MR and the interactions included. Since the QED effects are minor we may think of the differences in computed properties, to be discussed in the

coming sections, mainly in terms of the extended MR for the latter model. Once the ASFs have been obtained, the atomic parameters such as S and A can be calculated.

III. RESULTS

Some excitation energies (E) with the $J = 1$ in N⁺ as well as their relative differences with the experimental work ($\delta_E = \frac{|E_{\text{This}} - E_{\text{NIST}}|}{E_{\text{NIST}}}$) [38] are listed in Table II. The δ_E are controlled within 0.13% except for $2s2p^3\ ^3P_1^o$ (0.19%), $^3S_1^o$ (0.36%), $^1P_1^o$ (0.51%), and $2s2p^23s\ ^5P_1$ (0.26%). This signifies that our excitation energies are highly accurate and represent an improvement compared to Tayal's results [28]. The uncertainties of the rest of the states, i.e., the odd states of the $\{2s2p^3, 2s^22p3s, 2s^22p3d, 2s^22p4s, 2s^22p4d, 2s^22p5s\}$ configurations and the even states of the $\{2s^22p^2, 2s^22p3p, 2s^22p4p, 2s2p^23s, 2s^22p4f\}$ configurations, are further estimated within 0.13%, except for three states in $2s^22p^2$ [3P_2 (0.67%), 1D_2 (0.97%), 1S_0 (0.53%)]; four states in $2s2p^3$ [$^5S_2^o$ (1.01%), $^3P_{2,0}^o$ (0.19%), $^1D_2^o$ (0.58%)]; one state in $2s2p^23s$ [5P_3 (0.26%)] and two states in $2s^22p4p$ [1D_3 (0.26%), 1S_0 (0.29%)].

Accurate wavelengths (λ), line strengths (S), weighted oscillator strengths (gf) and A in Babushkin (length) gauge of some relatively strong intercombination lines, arising from $2s^2 2pnl$ ($n \geq 3$), are listed in Table III. Some other theoretical and experimental results are also listed using for comparison. Researchers often focus on that of $2s^2 2p3s-2s^2 2p3p$ and $2s^2 2p3p-2s^2 2p3d$ [10,11] as they are in visible region. Strong ultraviolet and infrared lines can be as characteristic lines, e.g., an exceptionally strong $\lambda 74.84$ nm [12], $\lambda 1386.647$ nm, etc. In diagnosing emission spectra of the earth and Titan, Tripp predicted the basic collision and radiative properties of N^+ , and gave radiative cooling coefficient [1]. However, their adopted data differ markedly from ours, e.g., the rate of $\lambda 74.837$ nm 4.8×10^8 s $^{-1}$ is nearly two times larger than our 2.71×10^8 s $^{-1}$. Ahmed and Sigut performed abundance studies using the Opacity Project data that are from non-relativistic calculations [8,41], and their diagnose would benefit from improved fully relativistic data.

The intercombination rates of $2s^2 2p^2-2s2p^3$ as well as the Branching Ratio (BR) $\frac{A_{\lambda 214.345}}{A_{\lambda 213.968}}$ are listed in Table IV, along with other theoretical and experimental results. The intercombination data of $2s^2 2p^2-2s2p^3$, especially for that of the extremely weak lines of $2s2p^3$ $^5S_2^o$ [$\lambda 213.968$ nm, $\lambda 214.345$ nm, and $\lambda 317.779$ nm] are also illustrated in Figs. 2(a)–2(c) below, have interesting applications in diagnosing Te and Ne of the Orion Nebula [1–3,7,8,13]. Musielok's experimental BR $\frac{A_{\lambda 214.345}}{A_{\lambda 213.968}}$ of $2s2p^3$ $^5S_2^o$ disagrees with others by about 9% [10]. It would be better if the experiment is improved. For a detailed discussion about the lines of $^5S_2^o$, their A , lifetimes, BR, applications, etc.; see Ref. [13].

IV. DISCUSSIONS

A. Electron correlation

Talay examined the importance of CV correlation by exciting one core $1s$ electron and one valence electron to other spectroscopic and correlation orbitals and found the effect to be small [28]. But things differ when CV is combined with CC correlations. Their effects can be reflected by the energy difference of $E_{7SDVC}-E_{7SDV}$ ($\Delta E_{CV\&CC}$). Table II shows that these correlations change most energies by 200 cm $^{-1}$ [13], except for $2s2p^3$ whose energies are changed from -450 cm $^{-1}$ to -1187 cm $^{-1}$. Talay has also examined the importance of CV correlation effects for the intercombination rates and found these to be insignificant [28]. However, important effects emerge if CV is included along with CC correlation. These effects and Breit interaction can be reflected using the changing tendency of rates in different models, i.e., $\frac{|A_X-A_{(X-1)}|}{A_{(X-1)}}$, where X is 7SDV, 7SDVC, 7SDVCB, 7SDVCBQ; ($X-1$) corresponds to 6SDV, 7SDV, 7SDVC, 7SDVCB. We illustrated them in Fig. 1, where three lines of $2s^2 2pns$ $^3P_1^o$ ($n = 3,4,5$) are selected. It is seen from the $\frac{|A_{7SDVC}-A_{7SDV}|}{A_{7SDV}}$ that CV and CC correlation effects change the A of a transition of lower excited states $2s^2 2p^2$ $^1D_2-2s^2 2p3s$ $^3P_1^o$ by 48.93%. These effects will gradually weaken for the A of the transitions of some highly excited states, $2s^2 2p3p$ $^1P_1-2s^2 2p4s$ $^3P_1^o$ and $2s^2 2p4p$ $^1P_1-2s^2 2p5s$ $^3P_1^o$, and become insignificant for the latter A .

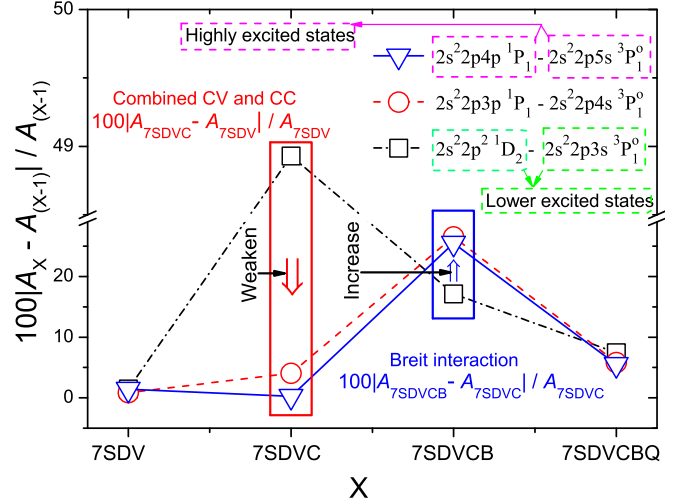


FIG. 1. The effects of combined CV and CC correlations as well as the Breit interaction on the intercombination rates. Y axis is the changing tendency of transition rates in different correlation models, i.e., $\frac{|A_X-A_{(X-1)}|}{A_{(X-1)}}$, where X is 7SDV, 7SDVC, 7SDVCB, 7SDVCBQ; ($X-1$) corresponds to 6SDV, 7SDV, 7SDVC, 7SDVCB.

There is a strong interaction between $2s2p^3$ $^1,3P_1^o$ and $2s^2 2p3s$ $^1,3P_1^o$ along with a strong spin-orbit mixing between the states $^3P_1^o$ and $^1P_1^o$ of $2s^2 2p3s$ [12,28]; see Table II. These make the levels sensitive to some remaining correlation effects [12,26,28]. In our calculation these are included through an extended MR $\{2s2p^3, 2s^2 2p3s, 2s^2 2p3d, 2s^2 2p4s, 2s^2 2p4d, 2s^2 2p5s\}$. This should be compared to the smaller MR $\{2s^2 2p3s, 2s2p^3\}$ and $\{2s^2 2p3s, 2s2p^3, 2s^2 2p3d\}$ of Ellis [12] and Tayal [28], respectively. A careful inspection shows that the extended MR gives rise to several CSFs with comparatively large mixing coefficients.

B. Breit interaction

The effect of Breit interaction is small for excitation energies, see the ΔE_{Breit} (or $E_{7SDVCB}-E_{7SDVC}$) in Table II. Intercombination rate is exception. It can be shown from the $\frac{|A_{7SDVCB}-A_{7SDVC}|}{A_{7SDVC}}$ in Fig. 1 that Breit interaction affects the A of $2s^2 2p^2$ $^1D_2-2s^2 2p3s$ $^3P_1^o$ by about 18%. For the transitions of some highly excited states the change is even larger. These large changes are in accordance with results for other near neutral systems. The underlying reason is the large cancellation effects for the transition matrix elements. Even small changes in the mixing coefficients for the CSFs due to the inclusion of the Breit interaction may have large effect. The situation is analyzed in detail by Ref. [30].

C. Intercombination transition rates

For the intercombination rates of $2s^2 2pnl$ ($n \geq 3$), Vaec pointed out [10,19] large discrepancies arise from intercombination rates of $2s^2 2p3s-2s^2 2p3p$ both in calculations and experiments. Table V(a) presents a obvious example by the rates of $2s^2 2p3s$ $^3P_1^o-2s^2 2p3p$ $^1P_1^o$. It is even more interesting to compare the calculated rates in intercombination and allowed cases. Both using CIV3, Vaec mentioned that their

TABLE V. (a) The A of some $2s^22p3s-2s^22p3p$ E1 lines as well as (b) their Branching Ratio (BR). (c) The uncertainties of intercombination rates ($100\delta_A$) of $2s^22pns-2s^22pnp$ ($n = 3, 4$). All the data of part (c) are listed according to the order from small gf to large one.

Lower	Upper	λ and gf		Present	CIV3		MCHF		Exp.
		$\lambda_{\text{Obs.}}^a$ (nm)	This- gf		Bell ^b	Vaeck ^c	Tayal ^d	Fischer ^e	
$2s^22p3s$	$2s^22p3p$				(a) A (s^{-1})				
$^3P_1^o$	1P_1	638.138	5.05[−2]	2.75[6]	1.95[6]	3.48[6]	4.45[6]	3.52[6]	4.9[6] ^f
$^1P_1^o$	1P_1	648.384	5.23[−1]	2.76[7]	2.86[7]	2.69[7]		2.58[7]	6.11 ± 0.7[6] ^g ; 3.33[7] ^f
				0.10	0.07	0.13		0.14	0.15 ^f
					(b) the BR of $\frac{A_{\text{intercombination}}}{A_{\text{allowed}}}$ (or $\frac{A_{\lambda 638.138}}{A_{\lambda 648.384}}$)				
$2s^22p3s$	$2s^22p3p$				(c) Uncertainties ($100\delta_A$)				
$^3P_0^o$	1P_1	636.855	1.65[−4]	5.06	0.20				
$^1P_1^o$	3P_1	466.851	1.72[−2]	5.61	3.93	2.02	14.73		
$^1P_1^o$	3S_1	507.501	2.05[−2]	2.06	9.66	8.77	6.20		
$^1P_1^o$	3P_0	467.622	2.09[−2]	5.74	4.39	2.34	16.32		
$^1P_1^o$	3P_2	465.583	2.30[−2]	6.35	6.82	4.15	17.42		
$^3P_1^o$	1S_0	340.911	2.38[−2]	3.77	3.29	1.24	1.40		
$^1P_1^o$	3D_1	576.905	2.78[−2]	4.52	4.74	11.64	4.20		
$^3P_1^o$	1P_1	638.138	5.05[−2]	5.19	6.58	8.81	6.54		
$^1P_1^o$	3D_2	574.889	5.90[−2]	4.30	5.28	10.74	4.30		
$^3P_1^o$	1D_2	395.697	1.04[−1]	4.13	13.26	14.84	0.33		
$2s^22p4s$	$2s^22p4p$								
$^3P_2^o$	1P_1	1831.807	3.10[−4]	25.12					
$^1P_1^o$	3P_0	1885.444	7.42[−4]	23.31	43.10				
$^3P_1^o$	1S_0	969.164	9.32[−4]	18.66	16.30				
$^3P_0^o$	1P_1	1776.073	1.32[−3]	2.49	6.68				
$^1P_1^o$	3D_2	2038.084	2.20[−3]	7.98	43.66				
$^1P_1^o$	3S_1	1760.883	4.00[−3]	6.92	15.38				
$^1P_1^o$	3P_1	1876.053	1.05[−2]	0.14	15.68				
$^1P_1^o$	3D_1	2059.550	1.70[−2]	3.63	9.45				
$^3P_1^o$	1P_1	1792.577	3.13[−2]	3.90	14.77				

^aReference [38].

^bReference [18].

^cReference [19].

^dTayal [28].

^eFischer and Tachiev [26].

^fMar *et al.* [11].

^gMusielok *et al.* [10].

allowed rates of $2s^22p3s-2s^22pnp$ ($n = 3, 4$) agree well with the ones of Bell's [18,19]. However, Vaeck's intercombination rates become about a factor two larger than that of Bell [18], only due to Vaeck's addition of $\{6s, 6p\}$ orbitals to the original $\{1s-5s, 2p-5p, 3d-5d, 4f\}$ orbital set of Bell. These can be also reflected by the BR of intercombination and allowed rates in Table V(b); e.g., Vaeck's $\frac{A_{\lambda 638.138}}{A_{\lambda 648.384}}$ is nearly two times larger than that of Bell. As mentioned in Sec. IV A, there is a strong spin-orbit mixing between the states $^3P_1^o$ and $^1P_1^o$ of $2s^22p3s$ [12,28]. It causes the intercombination rates on its states $^1,3P_1^o$ are exceedingly sensitive to electron correlations and other corrections. Under this case large discrepancies are produced in

calculations [12,18,19,26,28], e.g., the intercombination rates of $2s^22p^2-2s^22p3s$ $^1,3P_1^o$ and $2s^22p3s$ $^1,3P_1^o-2s^22p3p$ in Table V(a) and III. To estimate these theoretical uncertainties of the rates δ_A , we use the differences δ_S in line strength in length and velocity gauge and transition energy δ_E as suggested by Refs. [33,42],

$$\delta_A = \delta_E + \delta_S, \quad (4)$$

where

$$\delta_E = \frac{|E_{\text{calc}} - E_{\text{exp}}|}{\max(E_{\text{calc}}, E_{\text{exp}})}, \quad \delta_S = \frac{|S_{\text{len}} - S_{\text{vel}}|}{\max(S_{\text{len}}, S_{\text{vel}})}. \quad (5)$$

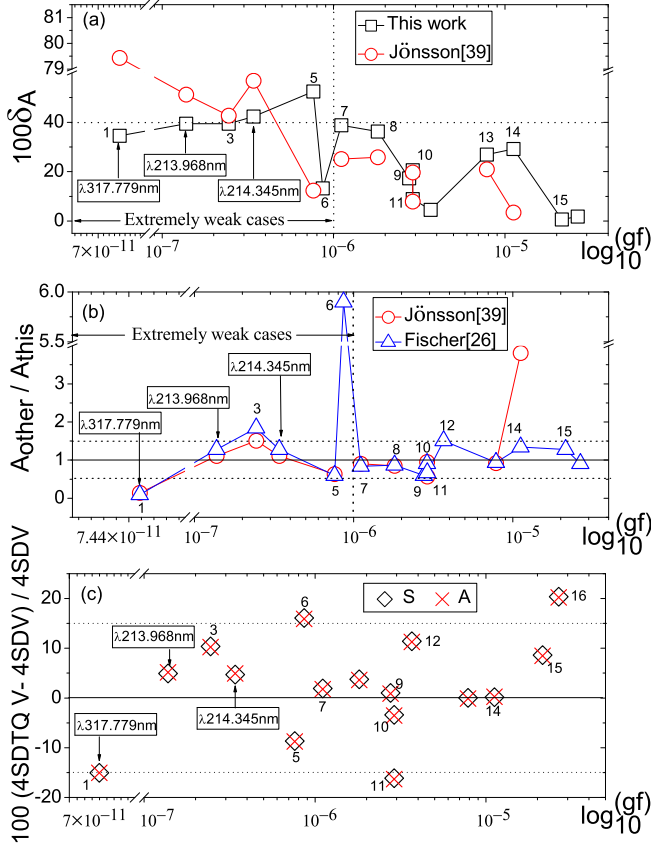


FIG. 2. (a) The uncertainties ($100\delta_A$) of intercombination A of $2s^22p^2-2s2p^3$ of N^+ . (b) The rate ratio $\frac{A_{\text{other}}}{A_{\text{this}}}$. (c) The assessments of the influences of some higher-order correlations. The tab “1,2, ...,16” from left to right in (a, b, c) indicates 16 lines of $2s^22p^2-2s2p^3$ listed in Table IV(a).

Table V(c) indicates our δ_A of $2s^22pns-2s^22pnp$ ($n = 3,4$) in $gf > 0.01$ case are better than others within 6.35% [18,19,28]. The rest δ_A of $2s^22p3l$ ($l = s,p,d$), $2s^22p4l$ ($l = s,p,d$) and $2s^22p5s$ in $gf > 0.01$ case are estimated by 7%, 12%, and 20%, respectively. The main reason of discrepancies is that cancellation effects in the transition matrix element make results very sensitive to both electron correlation and the Breit interaction [30]. In addition, other reasons are due to neglect of terms in the transition operator for the velocity gauge in non-relativistic calculations with Breit-Pauli corrections [26] and the neglect of contributions from the negative energy continuum for fully relativistic calculations using MCDHF [43,44]. Considering the stability and convergence in the Babushkin (length) gauge, this is the recommended gauge for transition data. Reseeing Table V(a), since two experimental results have large discrepancies to each other [10,11], even obviously are larger than other calculations, it would be better if they are improved.

The δ_A of intercombination rates of $2s^22p^2-2s2p^3$ are illustrated in Figs. 2(a) and 2(b). Jönsson and Bieroń have performed the rate calculations of $2s^22p^2-2s2p^3$, in which SD electrons were separately excited from $\{2s^22p^2, 2p^4\}$ and $\{2s2p^3\}$ to $\{n = 3, \dots, 8; l = s,p,d,f,g,h\}$. Some other correlation effects were further added in RCI calculations, where the MR for the terms of $2s^22p^2$ and $2s2p^3$ were sep-

arately enlarged to include $\{2s^22p^2, 2p^4, 2s2p^23d, 2s^23d^2\}$ and $\{2s2p^3, 2p^33d, 2s^22p3d, 2s2p3d^2\}$ [39]. The figure shows that the results of Jönsson [39], Fischer [26], and ours are in good agreement in cases $10^{-6} < gf < 0.01$, e.g., in Fig. 2(a) mostly $\delta_A < 40\%$, and most rate ratios in Fig. 2(b) are within 1 ± 0.5 . However, discrepancies become large for the extremely weak cases $gf < 10^{-6}$, e.g., in Fig. 2(a) the δ_A of $\lambda 317.779$ nm. This signifies that present models capture more correlation effects that are important for the rates. Because the rates are tiny at $10^2 s^{-1}$, some higher-order correlation effects become significant [13,29]. To estimate them we compute $\frac{100(A_{4SDTQV} - A_{4SDV})}{A_{4SDV}}\%$ where A_{4SDV} are the rates of the 4SDV model and A_{4SDTQ} are the rates of a model where also triple (T) and quadruple (Q) substitutions are allowed to the $\{2s-4s, 2p-4p, 3d-4d, 4f\}$ active set. Figure 2(c) displays that these higher-order correlation effects are controlled to within 15%, except for that of $\lambda 71.525$ nm (Tab-16) by about 20% for both S and A.

V. CONCLUSIONS

We show that CV and CC correlation effects are important for accurate predictions of energy levels and intercombination rates of N^+ . A strong spin-orbit mixing appears between the states $^3P_1^o$ and $^1P_1^o$ of $2s^22p3s$. It causes the intercombination rates on its states $^1,3P_1^o$ to be exceedingly sensitive to electron correlations and other corrections, e.g., that of $2s^22p^2-2s^22p3s$ $^1,3P_1^o$ and $2s^22p3s$ $^1,3P_1^o-2s^22p3p$. It is also found that the present models give rise to several CSFs with comparatively large mixing coefficients for the energy calculations of $2s^22p3s$ by extending the MR. Using a systematic procedure with increasing active orbital spaces, comparisons of the rates in length and velocity gauges and estimations of remaining correlation effects, it is possible to estimate the uncertainties. The uncertainties of intercombination rates of relatively strong lines ($gf > 0.01$) of $2s^22p3l$ ($l = s,p,d$), $2s^22p4l$ ($l = s,p,d$), and $2s^22p5s$ are separately estimated within 7%, 12%, and 20%. The strong intercombination lines in the visible region arise from $2s^22p3s-2s^22p3p$ and $2s^22p3p-2s^22p3d$. The present data, including that of strong infrared and ultraviolet intercombination lines, have potential applications in the diagnosis of radiative cooling coefficient, abundance, etc. The extremely weak transitions ($gf < 10^{-6}$) are difficult to accurately calculate, but are of interests in the temperature and density diagnostic in nebulae. The present model have included appropriate electron correlations to deal with them and provide guidance for future studies.

ACKNOWLEDGMENTS

We thank the financial support by the Research and Development Program for Science and Technology of Hebei Province (Grant No. 11217168), the Research and Development Program for Science and Technology of Handan (Grant No. 1523103064-6), the Science and Technology Research Project of University of Hebei Province (Grant No. ZC2016066), the National Natural Science Foundation of China (Grant No. 11164022), the Natural Science Foundation of Qinghai, China (Grant No. 2015-ZJ-948Q). P.J. acknowledge support from the Swedish research council under Contract No. 2015-04842.

- [1] T. M. Tripp, D. E. Shemansky, G. K. James, and J. M. Ajello, *Astrophys. J.* **368**, 641 (1991).
- [2] R. H. Rubin, P. G. Martin, R. J. Dufour, G. J. Ferland, J. A. Baldwin, J. J. Hester, and D. K. Walter, *Astrophys. J.* **495**, 891 (1998).
- [3] F. Keenan, F. L. Crawford, W. A. Feibelman, and L. H. Aller, *Astrophys. J. Suppl. Ser.* **132**, 103 (2001).
- [4] V. Escalante and C. Morisset, *Mon. Not. R. Astron. Soc.* **361**, 813 (2005).
- [5] C. E. Hudson and K. L. Bell, *Astron. Astrophys.* **436**, 1131 (2005).
- [6] Y. X. Guo, P. Yuan, X. Z. Shen, and J. Wang, *Phys. Scr.* **80**, 035901 (2009).
- [7] J. Y. Cen, P. Yuan, and S. M. Xue, *Phys. Rev. Lett.* **112**, 035001 (2014).
- [8] A. Ahmed and T. A. A. Sigut, *Mon. Not. R. Astron. Soc.* **455**, 1099 (2016).
- [9] B. C. Fawcett, *At. Data Nucl. Data Tables* **37**, 411 (1987).
- [10] J. Musielok, J. M. Bridges, S. Djurović, and W. L. Wiese, *Phys. Rev. A* **53**, 3122 (1996).
- [11] S. Mar, C. Perez, V. R. Gonzalez, M. A. Gigosos, J. A. D. Val, I. de la Rosa, and J. A. Aparicio, *Astron. Astrophys. Suppl. Ser.* **144**, 509 (2000).
- [12] D. G. Ellis, *Phys. Rev. A* **47**, 161 (1993).
- [13] X. Z. Shen, J. Liu, and F. Y. Zhou, *Mon. Not. R. Astron. Soc.* **462**, 1203 (2016).
- [14] H. G. Berry, W. S. Bickel, S. Bashkin, J. Désesquelles, and R. M. Schectman, *J. Opt. Soc. Am.* **61**, 947 (1971).
- [15] R. D. Knight, *Phys. Rev. Lett.* **48**, 792 (1982).
- [16] A. G. Calamai and C. E. Johnson, *Phys. Rev. A* **44**, 218 (1991).
- [17] E. Träbert, A. Wolf, E. H. Pinnington, J. Linkemann, E. J. Knystautas, A. Curtis, N. Bhattacharya, and H. G. Berry, *Phys. Rev. A* **58**, 4449 (1998).
- [18] K. L. Bell, A. Hibbert, and R. P. Stafford, *Phys. Scr.* **52**, 240 (1995).
- [19] N. Vaeck, J. Fleming, K. L. Bell, A. Hibbert, and M. R. Godefroid, *Phys. Scr.* **56**, 603 (1997).
- [20] X. Z. Shen, J. G. Li, P. Jönsson, and J. G. Wang, *Astrophys. J.* **801**, 129 (2015).
- [21] The Opacity Project Team, *The Opacity Project* (Institute of Physics, London, 1995), Vol. 1; <http://cdsweb.u-strasbg.fr/topbase/topbase.html>
- [22] A. Hibbert, *Phys. Scr.* **T65**, 104 (1996).
- [23] W. L. Wiese and J. R. Fuhr, *J. Phys. Chem. Ref. Data* **36**, 1287 (2007).
- [24] T. Brage, A. Hibbert, and D. S. Leckrone, *Astrophys. J.* **478**, 423 (1997).
- [25] C. Mendoza, C. J. Zeippen, and P. J. Storey, *Astron. Astrophys. Suppl. Ser.* **135**, 159 (1999).
- [26] C. F. Fischer and G. Tachiev, *At. Data Nucl. Data Tables* **87**, 1 (2004).
- [27] W. L. Wiese and J. R. Fuhr, *J. Phys. Chem. Ref. Data* **36**, 1737 (2007).
- [28] S. S. Tayal, *Phys. Rev. A* **83**, 012515 (2011).
- [29] C. F. Fischer, T. Brage, and P. Jönsson, *Computational Atomic Structure: An MCHF Approach* (Institute of Physics Publishing, Bristol/Philadelphia, 1997).
- [30] A. Ynnerman and C. F. Fischer, *Phys. Rev. A* **51**, 2020 (1995).
- [31] I. P. Grant, *Relativistic Quantum Theory of Atoms and Molecules: Theory and Computation* (Springer, Berlin, 2007).
- [32] C. F. Fischer, M. Godefroid, T. Brage, P. Jönsson, and G. Gaigalas, *J. Phys. B: At. Mol. Opt. Phys.* **49**, 182004 (2016).
- [33] J. Ekman, M. R. Godefroid, and H. Hartman, *Atoms* **2**, 215 (2014).
- [34] I. P. Grant, *J. Phys. B: At. Mol. Opt. Phys.* **7**, 1458 (1974).
- [35] C. F. Fischer and M. R. Godefroid, *Comput. Phys. Commun.* **64**, 501 (1991).
- [36] J. Olsen, M. R. Godefroid, P. Jönsson, P. A. Malmqvist, and C. F. Fischer, *Phys. Rev. E* **52**, 4499 (1995).
- [37] P. Jönsson, G. Gaigalas, J. Bieroń, C. F. Fischer, and I. P. Grant, *Comput. Phys. Commun.* **184**, 2197 (2013).
- [38] A. Kramida, Y. Ralchenko, and J. Reader, *Atomic Spectra Database (version 5.1)* (NIST ASD Team, National Institute of Standards and Technology, 2013); available at <http://physics.nist.gov/asd>
- [39] P. Jönsson and J. Bieroń, *J. Phys. B: At. Mol. Opt. Phys.* **43**, 074023 (2010).
- [40] J. M. Bridges, W. L. Wiese, and Griesmann, *Goddard High Resolution Spectrograph Science Symposium* (Greenbelt, MD, 1996).
- [41] D. Luo and A. K. Pradhan, *J. Phys. B: At. Mol. Opt. Phys.* **22**, 3377 (1989).
- [42] C. F. Fischer, *Phys. Scr.* **T134**, 014019 (2009).
- [43] P. Jönsson and C. F. Fischer, *Phys. Rev. A* **57**, 4967 (1998).
- [44] M. H. Chen, K. T. Cheng, and W. R. Johnson, *Phys. Rev. A* **64**, 042507 (2001).